

Valence states and metamagnetic phase transition in partially *B*-site-disordered perovskite $\text{EuMn}_{0.5}\text{Co}_{0.5}\text{O}_3$

A. N. Vasiliev,¹ O. S. Volkova,^{1,2} L. S. Lobanovskii,³ I. O. Troyanchuk,³ Z. Hu,⁴ L. H. Tjeng,⁴ D. I. Khomskii,⁴ H.-J. Lin,⁵ C. T. Chen,⁵ N. Tristan,⁶ F. Kretschmar,⁶ R. Klingeler,⁶ and B. Büchner⁶

¹*Moscow State University, Moscow 119991, Russia*

²*Institute of Radiotechnics and Electronics, RAN, Moscow 125009, Russia*

³*Institute of Solid State Physics and Semiconductors, NAS, Minsk 220072, Belarus*

⁴*II. Physikalisches Institut, Universität zu Köln, Zùlpischer Straße 77, 50937 Köln, Germany*

⁵*National Synchrotron Radiation Research Center, 101 Hsin-Ann Road, Hsinchu 30076, Taiwan*

⁶*Leibniz Institute for Solid State and Materials Research (IFW) Dresden, 01171 Dresden, Germany*

(Received 28 August 2007; revised manuscript received 18 January 2008; published 28 March 2008)

The valence states of transition metals were studied by measuring the x-ray absorption spectra at both Mn $L_{2,3}$ and Co $L_{2,3}$ edges of partially *B*-site-disordered perovskite $\text{EuMn}_{0.5}\text{Co}_{0.5}\text{O}_3$. By comparison with analogous spectra in various Co- and Mn-based compounds, the divalent state of the Co ions and the tetravalent state of the Mn ions were established analogous to $\text{Mn}^{4+}/\text{Co}^{2+}$ charge ordering found by Dass and Goodenough [Phys. Rev. B **67**, 014401 (2003)] in $\text{LaMn}_{0.5}\text{Co}_{0.5}\text{O}_3$. The specific heat and magnetic susceptibility data indicate the formation of the magnetically ordered state at $T_C \sim 120$ K. The first-order metamagnetic transitions seen in $\text{EuMn}_{0.5}\text{Co}_{0.5}\text{O}_3$ at $T < T_C$ suggest the existence of antiferromagnetic and/or paramagnetic clusters embedded into the ferromagnetic matrix.

DOI: [10.1103/PhysRevB.77.104442](https://doi.org/10.1103/PhysRevB.77.104442)

PACS number(s): 75.47.Lx, 75.60.Jk, 65.40.-b, 75.60.Ej

INTRODUCTION

Perovskites ABO_3 with mixed occupancy of the *B* site display a wider variety of physical phenomena when compared to traditional perovskites with mixed occupancy of the *A* site. In the former case, chemical substitution modifies the magnetically active subsystem of transition-metal ions. In the case of rare earth perovskites $\text{REM}_{1-x}\text{M}'_x\text{O}_3$, the physical properties are determined by the valence and spin states of the transition-metal ions *M* and *M'* as well as their interactions with each other and with the rare earth metal ions RE. The latter can be neglected when RE is a nonmagnetic ion as in the cases of RE=La, Eu, or Lu.

One of the most thoroughly studied systems of this type is $\text{LaMn}_{1-x}\text{Co}_x\text{O}_3$, whose basic properties have been established in pioneering works of Goodenough *et al.*¹ and Jonker.² It was assumed,¹ that Co^{3+} ions in $\text{LaMn}_{1-x}\text{Co}_x\text{O}_3$ are in the low-spin state ($d^6, S=0$) and the spontaneous magnetization is due to the ferromagnetic superexchange interaction of $\text{Mn}^{3+}\text{-O-Mn}^{3+}$ ($d^4, S=2$). The presence of transition-metal ions in different valence states (Mn^{3+} and Co^{3+} as well as Mn^{4+} and Co^{2+}) in $\text{LaMn}_{0.5}\text{Co}_{0.5}\text{O}_3$ was postulated in Ref. 2. In this case, spontaneous moment appears due to the ferromagnetic exchange interaction of $\text{Co}^{2+}\text{-O-Mn}^{4+}$. Based on x-ray absorption and photoemission spectroscopy, the data of Park *et al.*³ indicated the presence of Co^{2+} ions and explained the ferromagnetism in $\text{LaMn}_{1-x}\text{Co}_x\text{O}_3$ by $\text{Mn}^{3+}\text{-O-Mn}^{4+}$ double exchange interactions. The valence states of the transition-metal ions in this system were also discussed by Yang *et al.*,⁴ who concluded that there was no obvious mixed valence of $\text{Mn}^{3+}/\text{Mn}^{4+}$ obtained in the calculation.

Another aspect of the physics of the rare earth perovskites $\text{REM}_{1-x}\text{M}'_x\text{O}_3$ concerns nanoscale phase separation.⁵ It was shown⁶⁻⁸ that depending on synthesis conditions and thermal treatment, the $\text{LaMn}_{1-x}\text{Co}_x\text{O}_3$ system can adopt different

structural forms and exhibit a variety of different magnetic properties. In particular, the presence of enriched phases of Mn^{3+} and Co^{3+} as well as enriched phases of Mn^{4+} and Co^{2+} in $\text{LaMn}_{0.5}\text{Co}_{0.5}\text{O}_3$ was suggested. Various exchange interactions in this case were analyzed by Troyanchuk *et al.*⁹ Finally, multiple magnetic phases in oxygen deficient $\text{LaMn}_{0.5}\text{Co}_{0.5}\text{O}_{3-\delta}$ were studied and interpreted in Ref. 10 based on the hypothesis that the introduction of oxygen vacancies creates additional Mn^{3+} and intermediate Co^{3+} spins at neighboring sites around it. The important outcome of Ref. 10 was that the stoichiometric samples revealed perfect $\text{Mn}^{4+}/\text{Co}^{2+}$ charge ordering. A brief overview of the $\text{LaMn}_{1-x}\text{Co}_x\text{O}_3$ system indicates the rich physics possessed by these compounds in the presence of transition-metal ions in various valence and spin states.

The closest analog of the La-based system is the much less studied system of $\text{EuMn}_{1-x}\text{Co}_x\text{O}_3$ with nonmagnetic Eu^{3+} . The end compounds of this family are EuMnO_3 and EuCoO_3 . In EuMnO_3 , an incommensurate antiferromagnetic structure is formed at $T_{N1}=52$ K and an *A*-type antiferromagnetism is established at $T_{N2}=48$ K.¹¹ In contrast, EuCoO_3 is a nonmagnetic compound at low temperatures, the energy splitting in Co^{3+} ions between low spin ($S=0$) and the intermediate state ($S=1$) being estimated as 2200 K.¹² Starting from EuMnO_3 , the ferrimagnetic spin ordering temperature increases upon Co doping to a maximum value $T_C=120$ K in $\text{EuMn}_{0.5}\text{Co}_{0.5}\text{O}_3$ and decreases for higher Co concentrations.¹³

In the present work, the valence states of transition metals were studied by measurements of the x-ray absorption spectra (XAS) at both Mn $L_{2,3}$ and Co $L_{2,3}$ edges of partially *B*-site-disordered perovskite $\text{EuMn}_{0.5}\text{Co}_{0.5}\text{O}_3$. It was established that the lattice is formed mostly by divalent Co^{2+} (spin-only value $S=3/2$) and tetravalent Mn^{4+} ($S=3/2$) ions; the concentration of these ions in the other valence and spin

states is less than 10%. The measurements of magnetic susceptibility and specific heat of the pellet samples indicate that the compound experiences the transition into the magnetically ordered state at $T_C \sim 120$ K. This state exhibits both ferromagnetic and spin-glass features, the spin-glass component showing the first-order metamagnetic phase transitions in an external magnetic field.

EXPERIMENT

The pellet samples of $\text{EuMn}_{0.5}\text{Co}_{0.5}\text{O}_3$ were prepared by firing the starting mixture of Eu_2O_3 , Co_3O_4 , and Mn_2O_3 at 1000°C and sintering at $1250\text{--}1420^\circ\text{C}$, with subsequent cooling to room temperature at the rate of 100°C/h . Powder x-ray diffraction analysis shows that all the investigated samples are single phase. The structure of $\text{EuMn}_{0.5}\text{Co}_{0.5}\text{O}_3$ belongs to the orthorhombically distorted perovskite type. The oxygen content of the sample as measured by thermogravimetric analysis was found to exhibit a small oxygen excess so that the chemical formula reads $\text{EuMn}_{0.5}\text{Co}_{0.5}\text{O}_{3.02}$. The temperature and field dependences of the magnetization were measured by a Quantum Design MPMS superconducting quantum interference device (SQUID) magnetometer. For measurements in very small magnetic fields, a procedure of inductive coil demagnetization and compensating fields, respectively, have been applied. The specific heat data in the range $2\text{--}300$ K were obtained with the Quantum Design PPMS.

To clarify the valence states of Co and Mn ions in $\text{EuMn}_{0.5}\text{Co}_{0.5}\text{O}_3$, we measured XAS at both the Mn $L_{2,3}$ and Co $L_{2,3}$ edges of $\text{EuMn}_{0.5}\text{Co}_{0.5}\text{O}_3$. The Mn $L_{2,3}$ and Co $L_{2,3}$ XAS of $\text{EuMn}_{0.5}\text{Co}_{0.5}\text{O}_3$ were recorded at the Dragon beamline of the National Synchrotron Radiation Research Center in Taiwan with an energy resolution of 0.25 eV at the Co L_3 edge (≈ 780 eV). The CoO single crystals and the MnO single crystals were simultaneously measured for the Co $L_{2,3}$ spectra and the Mn $L_{2,3}$ spectra, respectively, in a separate chamber to obtain a relative energy reference with 0.05 eV accuracy. The samples were cleaved *in situ* at base pressures in the low 10^{-10} mbar region to obtain a clean sample surface. The spectra were recorded using the total electron-yield method.

The Co $L_{2,3}$ XAS of $\text{EuMn}_{0.5}\text{Co}_{0.5}\text{O}_3$ together with CoO as a divalent Co reference, EuCoO_3 as a low-spin (LS) trivalent Co reference, and $\text{Sr}_2\text{CoO}_3\text{Cl}$ as a high-spin (HS) trivalent Co reference¹⁴ are shown in Fig. 1. It is known that XAS, taken at the transition-metal $L_{2,3}$ edges, are highly sensitive to the valence state: an increase of the valence state of the metal ion by 1 causes a shift of the XAS $L_{2,3}$ by 1 or more eV toward higher energies.¹⁵ This shift is due to a final state effect in the x-ray absorption process. The energy difference between a $3d^n$ ($3d^7$ for Co^{2+}) and a $3d^{n-1}$ ($3d^6$ for Co^{3+}) configuration is $\Delta E = E(2p^6 3d^{n-1} \rightarrow 2p^5 3d^n) - E(2p^6 3d^n \rightarrow 2p^5 3d^{n+1}) \approx U_{pd} - U_{dd} \approx 1\text{--}2$ eV, where U_{dd} is the Coulomb repulsion energy between two $3d$ electrons and U_{pd} is the one between a $3d$ electron and the $2p$ core hole. In Fig. 1, a shift to higher energies by approximately 1.5 eV from divalent cobalt oxide CoO to both trivalent LS cobalt oxide EuCoO_3 and HS cobalt oxide $\text{Sr}_2\text{CoO}_3\text{Cl}$ is shown.

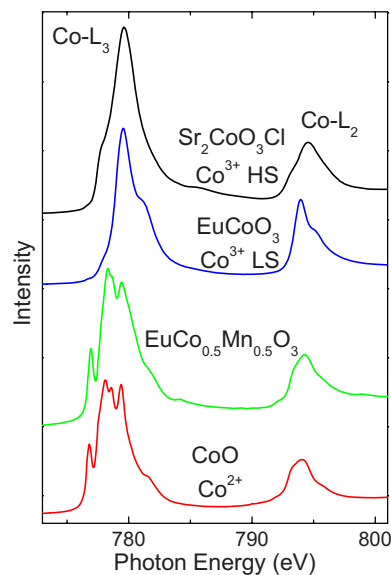


FIG. 1. (Color online) The Co $L_{2,3}$ XAS spectra of $\text{EuMn}_{0.5}\text{Co}_{0.5}\text{O}_3$ and the relevant spectra of CoO (Co^{2+}), EuCoO_3 (Co^{3+} low-spin state), and $\text{Sr}_2\text{CoO}_3\text{Cl}$ (Co^{3+} high-spin state).

The energy position and the spectral shape of $\text{EuMn}_{0.5}\text{Co}_{0.5}\text{O}_3$ are very similar to those of CoO, indicating an essentially divalent state of the Co ions in $\text{EuMn}_{0.5}\text{Co}_{0.5}\text{O}_3$. In fact, the detailed analysis of the Co $L_{2,3}$ spectral feature of $\text{EuMn}_{0.5}\text{Co}_{0.5}\text{O}_3$ allows one to suggest that it is very similar to the behavior of $\text{LaMn}_{0.5}\text{Co}_{0.5}\text{O}_3$ annealed in the temperature range $700\text{--}1300^\circ\text{C}$, where the combined experimental and theoretical studies on x-ray absorption spectra and x-ray magnetic circular dichroism measurements at the Co $L_{2,3}$ and the Mn $L_{2,3}$ edges indicate an essentially $\text{Co}^{2+}\text{--Mn}^{4+}$ valence state. At the increase of annealing temperature, the Co $L_{2,3}$ spectral feature of $\text{LaMn}_{0.5}\text{Co}_{0.5}\text{O}_3$ transforms in a way that suggests the appearance of Co^{3+} in a low-spin state.^{16,17}

For charge balance, we expect essentially a tetravalent state for the Mn ions in the $\text{EuMn}_{0.5}\text{Co}_{0.5}\text{O}_3$. To confirm these expectations, the Mn $L_{2,3}$ XAS were studied. Figure 2 shows the room temperature Mn $L_{2,3}$ XAS of $\text{EuMn}_{0.5}\text{Co}_{0.5}\text{O}_3$ together with MnO, LaMnO_3 , and SrMnO_3 (taken from Ref. 18) as divalent, trivalent, and tetravalent Mn references. A gradual shift to higher energies from MnO to LaMnO_3 and, further, to $\text{EuMn}_{0.5}\text{Co}_{0.5}\text{O}_3$, indicating an increase of the Mn valence state from $2+$ to $3+$ and, further, to $4+$, respectively, is seen. The spectral feature of Mn $L_{2,3}$ of $\text{EuMn}_{0.5}\text{Co}_{0.5}\text{O}_3$ is the same as that of $\text{EuMn}_{0.5}\text{Ni}_{0.5}\text{O}_3$,¹⁹ in which a $\text{Ni}^{2+}/\text{Mn}^{4+}$ valence state was found from both Ni $L_{2,3}$ and Mn $L_{2,3}$ XAS. The overall Mn $L_{2,3}$ spectral feature of $\text{EuMn}_{0.5}\text{Ni}_{0.5}\text{O}_3$ is very similar to that of $\text{LaMn}_{0.5}\text{Co}_{0.5}\text{O}_3$ with $T_C = 225$ K. Thus, the Mn $L_{2,3}$ XAS further confirms a Mn^{4+} state in the $\text{LaMn}_{0.5}\text{Co}_{0.5}\text{O}_3$ phase.

The temperature dependence of the specific heat c_p of $\text{EuMn}_{0.5}\text{Co}_{0.5}\text{O}_3$, shown in Fig. 3, indicates a phase transition at $T_C \sim 120$ K which is in good agreement with the previously published magnetization data.¹³ At room temperature, the specific heat c_p apparently reaches the thermodynamic limit $3Rn = 124.71$ J/mol K of the lattice contribution to the

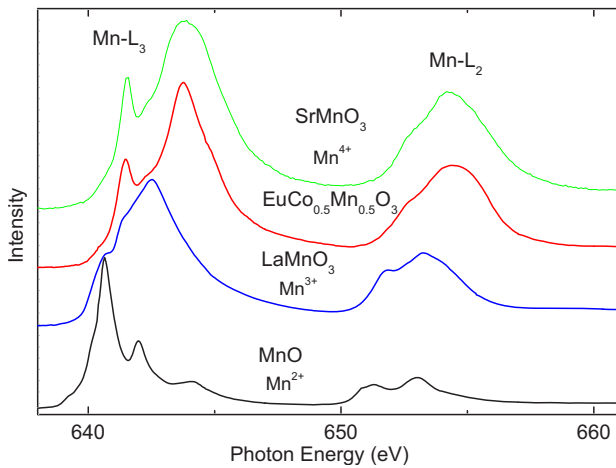


FIG. 2. (Color online) The Mn $L_{2,3}$ XAS spectra of $\text{EuMn}_{0.5}\text{Co}_{0.5}\text{O}_3$ and the relevant spectra of MnO (Mn^{2+}), LaMnO_3 (Mn^{3+}), and SrMnO_3 (Mn^{4+}).

entropy, with R being the gas constant and n the number of ions per unit cell. This, however, does not indicate an unusually small Debye temperature, but rather implies a significant electronic or/and magnetic contribution to the heat capacity at elevated temperatures. The Debye temperature Θ_D estimated from the C vs T curve in the range 2–20 K amounts to 345 ± 15 K. This value should be considered as a rough estimation only, since the contributions from electronic and magnetic subsystems are present in the heat capacity of the sample at low temperatures. Note that no other appreciable anomalies besides that at T_C are seen in c_p vs T in the temperature range studied.

The temperature dependences of the reduced magnetization M/H in $\text{EuMn}_{0.5}\text{Co}_{0.5}\text{O}_3$, taken in FC measurements in various magnetic fields, are shown in Fig. 4. These dependences indicate an evolvement of a ferromagnetic moment at $T_C \sim 120$ K. The reduced magnetization monotonically increases upon cooling, but shows a tendency to saturate at the lowest temperatures. The temperature dependence of the static susceptibility in the paramagnetic range is shown in the inset of Fig. 4. Since the samples studied were found to be

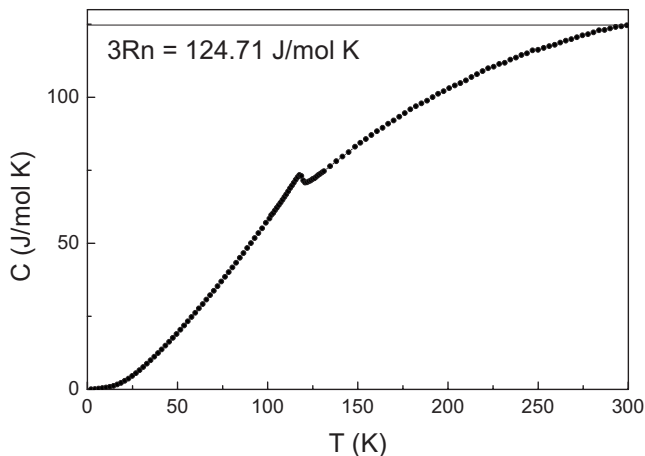


FIG. 3. The temperature dependence of the specific heat of $\text{EuMn}_{0.5}\text{Co}_{0.5}\text{O}_3$.

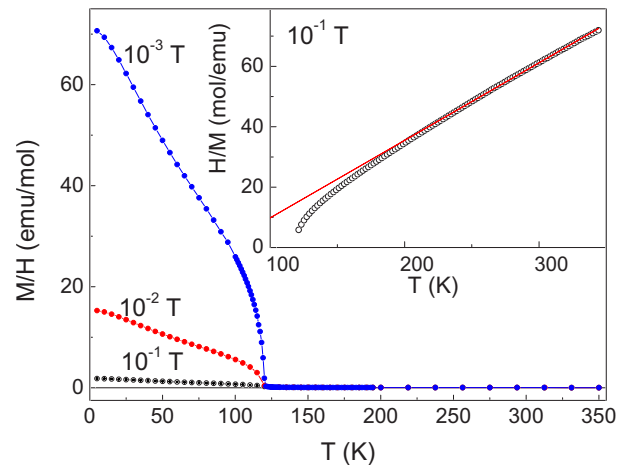


FIG. 4. (Color online) The temperature dependences of the reduced magnetization of $\text{EuMn}_{0.5}\text{Co}_{0.5}\text{O}_3$ measured in the FC mode in various magnetic fields. The inset represents the temperature dependence of the inverse magnetic susceptibility in the paramagnetic state taken at 0.1 T. The straight line is the Curie–Weiss law.

very sensitive to the minor magnetic fields trapped in a superconducting solenoid of a MPMS SQUID magnetometer (cf. Tung *et al.*²⁰), the measurements in the zero-field-cooled regime were not possible to perform in a reproducible manner. Instead, we made measurements after cooling in well defined, either positive or negative, magnetic field $\pm 10^{-4}$ T. The results of this study are shown in Fig. 5. The comparison of these curves clearly reveals the spin-glass-like behavior.

The temperature dependence of the magnetic susceptibility in the paramagnetic state obeys the Curie–Weiss (CW) law,

$$\chi(T) = \chi_0 + \frac{C}{T - \Theta_{\text{CW}}}.$$

Fitting the data yields a temperature independent term $\chi_0 = 2.2 \times 10^{-3}$ emu/mol, the Curie–Weiss constant $C = 3$ K emu/mol, and the Curie–Weiss temperature $\Theta_{\text{CW}} = 88$ K.

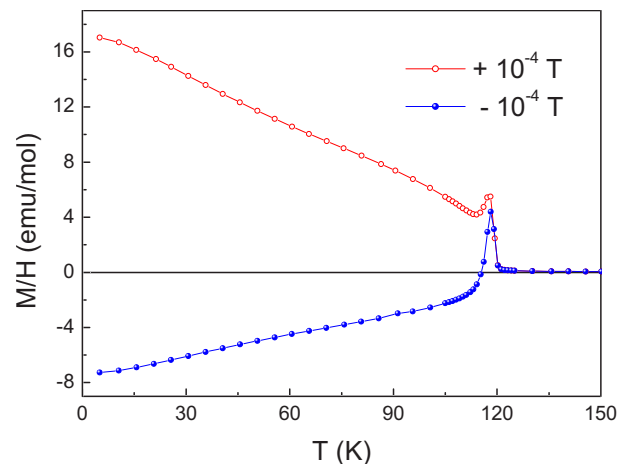


FIG. 5. (Color online) The temperature dependences of the reduced magnetization of $\text{EuMn}_{0.5}\text{Co}_{0.5}\text{O}_3$ taken after cooling in either positive or negative magnetic field $\pm 10^{-4}$ T.

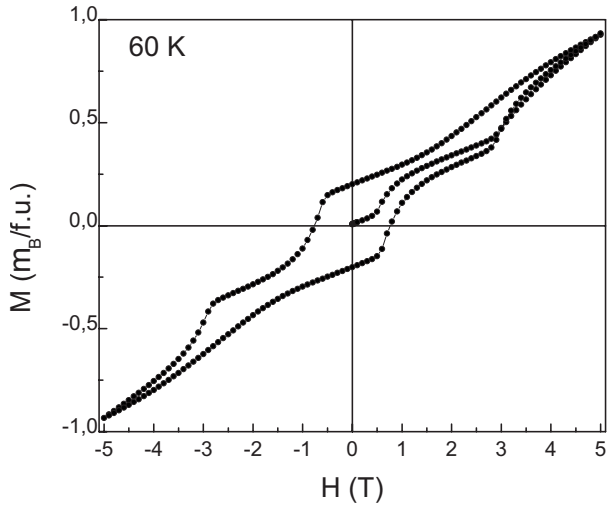


FIG. 6. The hysteresis loop in $\text{EuMn}_{0.5}\text{Co}_{0.5}\text{O}_3$ measured at 60 K after cooling at 10^{-3} T.

The unusually large value of the temperature independent term could be attributed to the presence of a significant van Vleck contribution of the Eu^{3+} ions. The obtained Curie–Weiss constant at high temperatures C implies $\mu_{\text{eff}} = 4.9 \mu_B/\text{f.u.}$, with μ_{eff} being the effective magnetic moment. This moment is comprised of effective magnetic moments of manganese and cobalt ions:

$$\mu_{\text{eff}}^2 = 0.5\mu_B^2 [g_{\text{Mn}}^2 S_{\text{Mn}}(S_{\text{Mn}} + 1) + g_{\text{Co}}^2 S_{\text{Co}}(S_{\text{Co}} + 1)].$$

The spin-only values S of the magnetic moments of Co^{2+} and Mn^{4+} ions are $3/2$. The g factor of manganese can be assumed to be close to 2, while for the cobalt ions, significantly larger values of the g factor are observed usually due to the orbital contribution.²¹ In the assumption of Co^{2+} and Mn^{4+} valence states, the value of the effective magnetic moment per formula unit obtained corresponds to $g_{\text{Co}}=3$. The thermogravimetric analysis of the sample studied revealed a small oxygen excess. Assuming only Mn^{4+} state, both in the bulk and at the grain boundaries, the amount of 8% of Co^{3+} in the low-spin state is expected. This will change the estimation for the g factor of Co^{2+} to $g_{\text{Co}}=3.1$.

The positive value of Θ_{CW} points to dominating ferromagnetic interactions. However, we find $\Theta_{\text{CW}} < T_C$ despite the fact that quantum fluctuations usually result in a reduction of the spin ordering temperature compared to the mean field prediction. We assume a competition of ferromagnetic and antiferromagnetic exchange interactions in the system to be responsible for this behavior. In addition, fluctuations are supposed to yield a noticeable deviation of the experimental data from the Curie–Weiss law when approaching T_C , which indeed is observed in our data.

The hysteresis loop of the magnetization M in $\text{EuMn}_{0.5}\text{Co}_{0.5}\text{O}_3$ measured at 60 K after cooling in the FC mode at $B=10^{-4}$ T is shown in Fig. 6. The data demonstrate features similar to metamagnetic transitions and show a large remanent magnetization M_{rem} . Evidently, there are kinks in M vs B , which indicate a steplike increase of the magnetization. We find that the critical field of the metamagnetic tran-

sition does not depend on the magnetic history of the sample and that the saturation magnetization M_{sat} is not reached at 5 T, which is the maximum field used in the experiment. At increasing temperature, the critical field of the metamagnetic transition monotonically decreases and turns to zero at T_C .

DISCUSSION

The x-ray absorption spectra at both Co $L_{2,3}$ and Mn $L_{2,3}$ of $\text{EuMn}_{0.5}\text{Co}_{0.5}\text{O}_3$ give clear evidence that the main valence states of the transition metals in this compound are Co^{2+} and Mn^{4+} . The probability of the presence of Co and Mn in other valence states in the sample studied is estimated to be less than 10%. However, the explanation of the whole set of experimental data on field and temperature dependences of magnetization demands the presence of disorder, i.e., the formation of some amount of antisite defects in the valence state that are the same or different from that of the host lattice. In the absence of a direct experimental confirmation on the presence of cobalt and manganese ions in the valence states different from that in the host matrix, we can refer only to the results of structural refinement in isostructural $\text{TbMn}_{0.5}\text{Co}_{0.5}\text{O}_3$ (Ref. 22) and $\text{NdCo}_{0.5}\text{Mn}_{0.5}\text{O}_3$ (Ref. 23) compounds. Based on the results of neutron powder diffraction in these compounds, about 1/3 of transition-metal ions occupy the antisite positions in the structure as opposed to almost complete transition-metal ion ordering in $\text{LaMn}_{0.5}\text{Co}_{0.5}\text{O}_3$.¹⁰

The formation of antisite defects may cause the valence and spin states of the transition-metal ions to change so that the system could accommodate elastic strains in the crystal lattice. We presume that when the large high-spin Co^{2+} ions (88.5 pm) replace significantly smaller Mn^{4+} ions (67 pm), they are losing one electron per ion to acquire the smaller radii of either low-spin Co^{3+} (68.5 pm) or high-spin Co^{3+} (75 pm). Therefore, manganese is forced to acquire one extra electron per ion and, thus, transforms to the high-spin Mn^{3+} state (78.5 pm).

Under the assumption that the exchange interaction between Co^{2+} and Mn^{4+} in the host matrix is ferromagnetic, the appearance of these ions in antisite positions will be accompanied by the establishment of strong Co^{2+} – Co^{2+} and weaker Mn^{4+} – Mn^{4+} antiferromagnetic interactions. By changing the valence state of cobalt in antisite positions, the antiferromagnetic interaction is either preserved (Co^{2+} –high-spin Co^{3+}) or vanishes (Co^{2+} –low-spin Co^{3+}). Accordingly, by changing the valence state of manganese in antisite positions, the ferromagnetic interaction Mn^{3+} – Mn^{4+} may appear. This wide spectrum of possible signs and magnitudes of exchange interaction favors the formation of a spin-glass-like state consisting of a ferromagnetic matrix and antiferromagnetic or paramagnetic clusters. The nonequivalence of the parameters of various exchange interactions in the system, along with different values of Co^{2+} (spin-only value $S=3/2$), Mn^{4+} ($S=3/2$), and Mn^{3+} ($S=2$) magnetic moments, results in a severe deformation of the Brillouin function of $\text{EuMn}_{0.5}\text{Co}_{0.5}\text{O}_3$, as seen in Figs. 4 and 5.

The scenario of separation into phases with different Curie temperatures can be excluded based on the absence of any

appreciable anomalies in the measured specific heat of $\text{EuMn}_{0.5}\text{Co}_{0.5}\text{O}_3$ at temperatures both above and below T_C . According to the results of thermodynamic characterization of $\text{EuMn}_{0.5}\text{Co}_{0.5}\text{O}_3$, the sample consists of ferromagnetic and spin-glass-like phases. The former phase corresponds to the host lattice with ferromagnetic exchange interaction of $\text{Co}^{2+}\text{-O-Mn}^{4+}$. In the disordered phase, the competition between ferromagnetic $\text{Co}^{2+}\text{-O-Mn}^{4+}$ and antiferromagnetic $\text{Co}^{2+}\text{-O-Co}^{2+}$ and $\text{Mn}^{4+}\text{-O-Mn}^{4+}$ exchange interactions as well as the presence of diamagnetic Co^{3+} ions lead to the formation of the spin-glass-like state. Based on the magnetization loop shown in Fig. 6, one can presume that the spin-glass-like phase transforms into a ferromagnetic phase under an external magnetic field via the succession of metamagnetic transitions with a large hysteresis, which clearly indicates their first-order nature.²⁴

In conclusion, the study of x-ray absorption spectra at both Co $L_{2,3}$ and Mn $L_{2,3}$ edges of $\text{EuMn}_{0.5}\text{Co}_{0.5}\text{O}_3$ provides a firm basis for the understanding of the peculiar magnetic

properties of this compound. Our study of specific heat and magnetization is in agreement with the suggestion that the samples studied consist of antiferromagnetic and/or paramagnetic clusters with different degrees of antisite defects of the Co and Mn ions, embedded into the ferromagnetic matrix. The magnetic response of this compound exhibits both ferromagnetic and spin-glass effects. The application of an external magnetic field leads to a transformation of the spin-glass component into the ferromagnetic one via the first-order metamagnetic phase transition.

ACKNOWLEDGMENTS

Support by the Deutsche Forschungsgemeinschaft (DFG) under Contracts No. 486 RUS 113/864/0-1, No. HE 3439/1, No. KL 1824, and No. SFB 608, and by the RFBR-BRFBR program under Grants No. 06-02-81021 and No. 07-02-91201 is gratefully acknowledged.

-
- ¹J. B. Goodenough, A. Wold, R. J. Arnett, and N. Menyuk, *Phys. Rev.* **124**, 373 (1961).
²G. H. Jonker, *J. Appl. Phys.* **37**, 1424 (1966).
³J.-H. Park, S.-W. Cheong, and C. T. Chen, *Phys. Rev. B* **55**, 11072 (1997).
⁴Z. Yang, L. Ye, and X. Xie, *Phys. Rev. B* **59**, 7051 (1999).
⁵E. Dagotto, *Nanoscale Phase Separation and Colossal Magnetoresistance* (Springer-Verlag, Berlin, 2003).
⁶P. A. Joy, Y. B. Khollam, and S. K. Date, *Phys. Rev. B* **62**, 8608 (2000).
⁷V. L. Joseph Joly, P. A. Joy, S. K. Date, and C. S. Gopinath, *J. Phys.: Condens. Matter* **13**, 649 (2001).
⁸V. L. Joseph Joly, P. A. Joy, and S. K. Date, *Solid State Commun.* **121**, 219 (2002).
⁹I. O. Troyanchuk, L. S. Lobanovsky, D. D. Khalyavin, N. S. Pastushonok, and H. Szymczak, *J. Magn. Magn. Mater.* **210**, 63 (2000).
¹⁰R. I. Dass and J. B. Goodenough, *Phys. Rev. B* **67**, 014401 (2003).
¹¹T. Goto, T. Kimura, G. Lawes, A. P. Ramirez, and Y. Tokura, *Phys. Rev. Lett.* **92**, 257201 (2004).
¹²J. Baier, S. Jodlauk, M. Kriener, A. Reichl, C. Zobel, H. Kierpel, A. Freimuth, and T. Lorenz, *Phys. Rev. B* **71**, 014443 (2005).
¹³I. O. Troyanchuk, D. D. Khalyavin, J. W. Lynn, R. W. Erwin, Q. Huang, H. Szymczak, R. Szymczak, and M. Baran, *J. Appl. Phys.* **88**, 360 (2000).
¹⁴Z. Hu, H. Wu, M. W. Haverkort, H. H. Hsieh, H. J. Lin, T. Lorenz, J. Baier, A. Reichl, I. Bonn, C. Felser, A. Tanaka, C. T. Chen, and L. H. Tjeng, *Phys. Rev. Lett.* **92**, 207402 (2004).
¹⁵C. Mitra, Z. Hu, P. Raychaudhuri, S. Wirth, S. I. Csiszar, H. H. Hsieh, H.-J. Lin, C. T. Chen, and L. H. Tjeng, *Phys. Rev. B* **67**, 092404 (2003).
¹⁶V. L. Joly, Y. B. Khollam, P. A. Joly, C. S. Gopinath, and S. K. Date, *J. Phys.: Condens. Matter* **13**, 11001 (2001).
¹⁷T. Burnus (private communication).
¹⁸R. K. Sahu, Z. Hu, M. L. Rao, S. S. Manoharan, T. Schmidt, B. Richter, M. Knupfer, M. Golden, J. Fink, and C. M. Schneider, *Phys. Rev. B* **66**, 144415 (2002).
¹⁹M. C. Sanchez, J. Garcia, J. Blasco, G. Subias, and J. Perez-Cacho, *Phys. Rev. B* **65**, 144409 (2002).
²⁰L. D. Tung, M. R. Lees, G. Balakrishnan, and D. McKPaul, *Phys. Rev. B* **75**, 104404 (2007).
²¹A. Abragam and B. Bleaney, *EPR of Transition Ions* (Clarendon, Oxford, 1970).
²²V. A. Khomchenko, I. O. Troyanchuk, A. P. Sazonov, V. V. Sikolenko, H. Szymczak, and R. Szymczak, *J. Phys.: Condens. Matter* **18**, 9541 (2006).
²³A. P. Sazonov, I. O. Troyanchuk, V. V. Sikolenko, H. Szymczak, and K. Baerner, *Phys. Status Solidi B* **244**, 3367 (2007).
²⁴A. P. Sazonov, I. O. Troyanchuk, M. Kopcewicz, V. V. Sikolenko, U. Zimmermann, and K. Bärner, *J. Phys.: Condens. Matter* **19**, 046218 (2007).